ELSEVIER

Journal of Nuclear Materials 296 (2001) 1–16

journal of nuclear materials

www.elsevier.com/locate/jnucmat

Section 1. General

R&D for the Spallation Neutron Source mercury target

L.K. Mansur *, T.A. Gabriel, J.R. Haines, D.C. Lousteau

Oak Ridge National Laboratory, P.O. Box 2008, Oak Ridge, TN 37831-6151, USA

Abstract

An overview of the research and development program for the Spallation Neutron Source (SNS) is presented. The materials-related efforts in target development are emphasized in order to provide a perspective for a number of specialized papers that are included in these proceedings. We give a brief introduction and historical sketch of the SNS project. Part of the materials R&D consists of calculations of radiation damage and of transmutation rates. He and H are considered to be the most important transmutation products. Radiation effects and Hg compatibility investigations make up the major part of the experimental effort. In the former, spallation irradiations are carried out in the LANSCE at Los Alamos National Laboratory and in the SINQ at the Paul Scherrer Institute. Irradiations that simulate aspects of a spallation environment are included to extend the parameter space of the spallation irradiations. The simulations are carried out at the low energy (MeV) accelerators of the TIF facility and at the HFIR reactor, both located at Oak Ridge National Laboratory. Irradiated specimens are tested for changes in mechanical properties and are characterized with respect to microstructural changes by transmission electron microscopy. The compatibility experiments cover both the effects of Hg on behavior in mechanical properties tests, and the effects of flowing Hg on mass transfer in target structural materials. The results of this extensive program of materials work indicate that the target design and materials performance will meet their intended service. Published by Elsevier Science B.V.

1. Introduction

The Spallation Neutron Source (SNS) is being designed as an accelerator-based neutron source that provides pulsed beams of spallation neutrons by bombarding a mercury target with 1 GeV protons. The primary purpose of the facility is to produce intense pulsed beams of neutrons for research in materials science and condensed matter physics. The facility will fulfill the needs of the neutron-scattering community well into this century. The project is a cooperative venture among six laboratories: Argonne National Laboratory, Brookhaven National Laboratory, Jefferson Laboratory, Lawrence Berkeley National Laboratory, Los Alamos National Laboratory (LANL), and Oak Ridge National Laboratory. The SNS is located at ORNL, which manages the project and is responsible for engineering the target station.

In the broadest terms, the facility consists of an ion source, a linear accelerator, a proton storage ring, and a target station. The target station includes the mercury target, neutron moderators, neutron beam tubes and neutron scattering instruments. The target is positioned within an iron and concrete shielding monolith approximately 12 m in diameter. Fig. 1 gives the overall layout of the facility, showing the accelerator and target station. Fig. 2 shows a cutaway view of the target and beam-tube region.

A heavy liquid–metal target was selected in preference to a water-cooled solid target for several reasons. Some advantages include higher neutron production, increased heat removal capability, and the absence of radiation damage to the target material itself. The heavy liquid metal target concept was initially suggested as a result of a technical study for the European Spallation Source (ESS) [1,2]. The target container material will, however, experience radiation damage. The spallation target is at the heart of the facility and performance of the container material is crucial to the successful operation of the SNS.

* Corresponding author. Tel.: +1-865 574 4797; fax: +1-865 574 0641.

E-mail address: mansurlk@ornl.gov (L.K. Mansur).

0022-3115/01/$ - see front matter. Published by Elsevier Science B.V.
PII: S 0 0 2 2 - 3 1 1 5 (0 1) 0 0 5 6 0 - 8

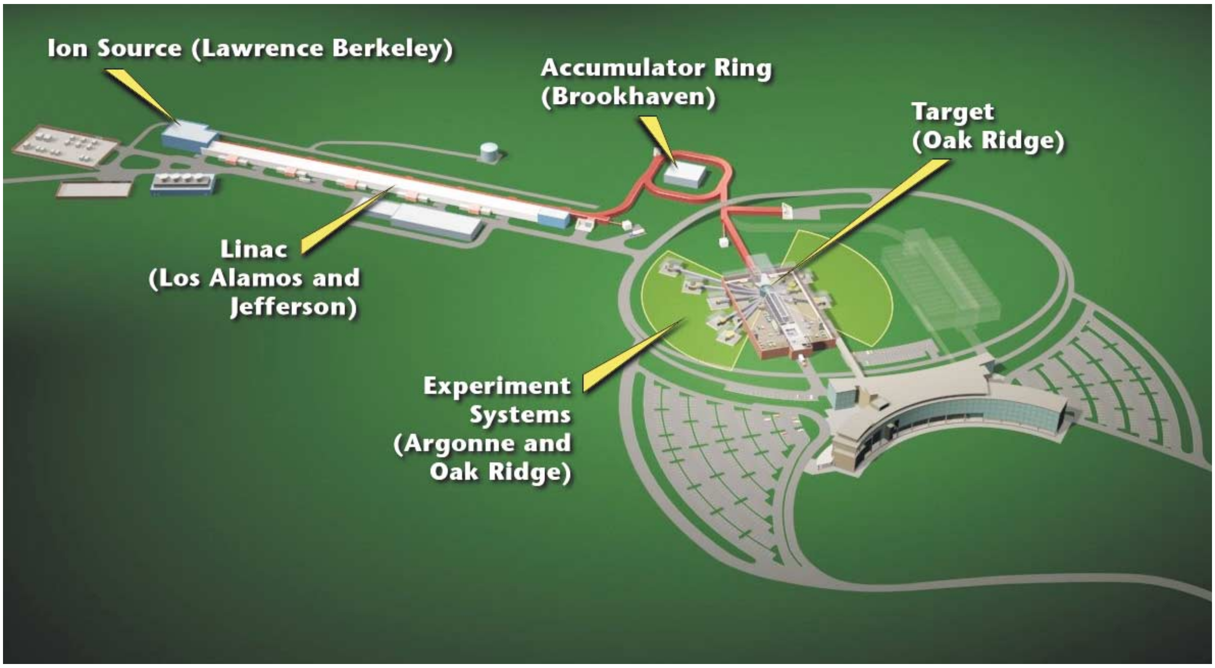

Fig. 1. Artist's conception of the layout of the SNS, showing the main accelerator and target systems. The six US laboratories participating in the project are identified with the systems for which they are primarily responsible.

2. Background

The SNS is currently the largest civilian science project in the USA. It is funded by the US government through its Department of Energy. The total projected cost is approximately $1.4 B. The multi-laboratory approach to construction was chosen because of the different types of expertise needed for major components of the project, and the existing distributed nature of this expertise across laboratories.

Preliminary planning was initiated in 1995. An R&D program was developed to provide the knowledge necessary for confident design and engineering of major systems. In particular, the materials R&D program for the target, which is of main interest in the present proceedings, was initiated at the very earliest stage. A conceptual design was produced by 1997 [3]. The critical decision to begin construction was made on November 5, 1999, and groundbreaking took place on December 15, 1999. Today, detailed design is approaching completion and large-scale construction is underway. Operation is scheduled to begin in 2006.

The present international series of meetings, the International Workshops on Spallation Materials Technology, was begun in April 1996 in Oak Ridge, TN. A proceedings containing summaries and presentation materials of the speakers was produced [4]. Subsequent workshops of the series were held in Ancona, Italy, September 1997 and Santa Fe, New Mexico, April 1999. The respective proceedings of these meetings [5,6] also contained summaries and presentation materials of the speakers. For the present workshop the proceedings are being published as full papers because of the rapid progression of the work and the burgeoning wealth of results and analyses. Two earlier workshops may also be thought of as an informal part of the present series. One, entitled Materials for Spallation Neutron Sources, was organized by LANL and held at Los Alamos, New Mexico, February 1995. It did not publish a proceedings but issued a summary report [7]. The other, entitled International Workshop on the Technology and Thermal Hydraulics of Heavy Liquid Metals, organized by the Paul Scherrer Institute and ORNL and held at Schruns, Austria, March 1996, prioritized the selection of liquid metal candidates and examined the technology, including materials technology, to develop these as the basis of spallation targets [8].

3. SNS target design

The SNS target system must be capable of receiving a 1 GeV proton beam with a time-averaged power level of up to 2 MW produced by 695 ns, 33.3 kJ pulses at frequencies up to 60 Hz. The system, shown in Fig. 3, is comprised of the following: a stainless steel structure containing mercury, referred to as the target module, that is placed in the path of the proton beam for pro-

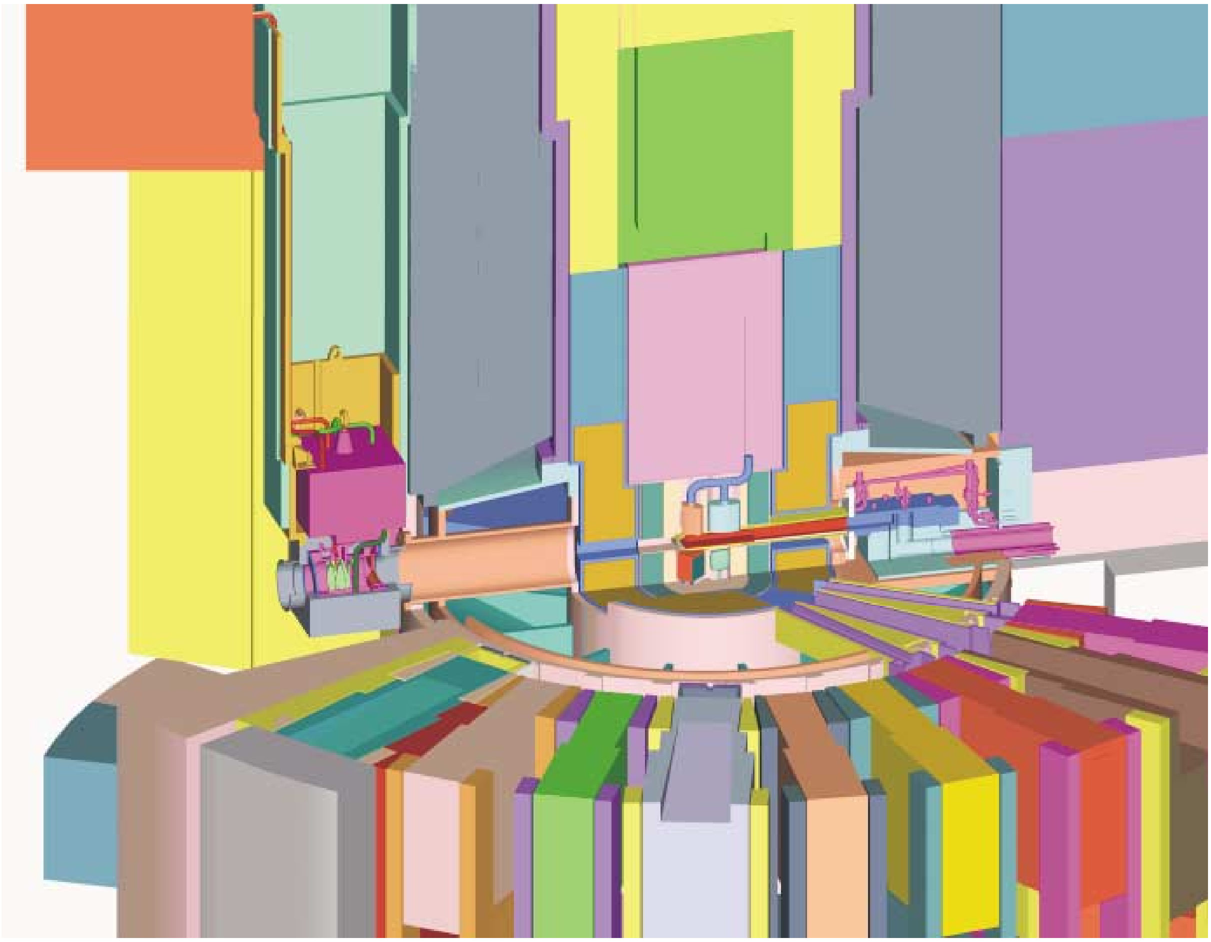

Fig. 2. Cutaway representation of the target area. Target, moderators, and shielding are the key components shown.

duction of neutrons; a process loop for safely transferring the power absorbed in the mercury from its interactions with the proton beam and resulting nuclear radiation to secondary cooling systems; a means for moving the target module between its installed position and a hot cell, where it can be maintained and replaced at the end of its useful life; moveable shielding in the target module's path between the hot cell and its installed position.

The target module, shown in Fig. 4, includes the mercury vessel, the water-cooled shroud, and seals mounted on a flange that form the interface to the core vessel and process piping. The mercury target vessel is comprised of front and rear sections connected by flow tubes. The front section is located within the core vessel during operation, i.e. forward of the seal between the target and vessel. The rear section, behind the seal, contains the joint used for disconnecting the target module from the piping in the plug. Every target change includes a new set of seals.

The front section contains the mercury that absorbs the proton beam energy and experiences the highest level of heat and neutron flux. As shown in Fig. 5, a vertical center cross-section of the front end of the module parallel to the direction of the beam, a dedicated of flow of mercury is directed between the walls of the mercury vessel in order to cool the target window, the portion of the vessel in the direct path of the proton beam. A cross-section of the module perpendicular to the proton beam is shown in Fig. 6. A separate flow of bulk mercury enters from two side regions outside of the beam and returns through the center portion of the vessel. Besides serving as flow guides, the baffle plates used to separate the inlet and outlet flow streams support the upper and lower flat plates, reducing the thickness of these plates needed to contain the internal pressure. The use of two separate flow streams is judged to be more predictable, reliable, and efficient (high convective heat transfer rates with minimal pumping power losses) than using the bulk mercury to cool the window. Also, the duplex structure

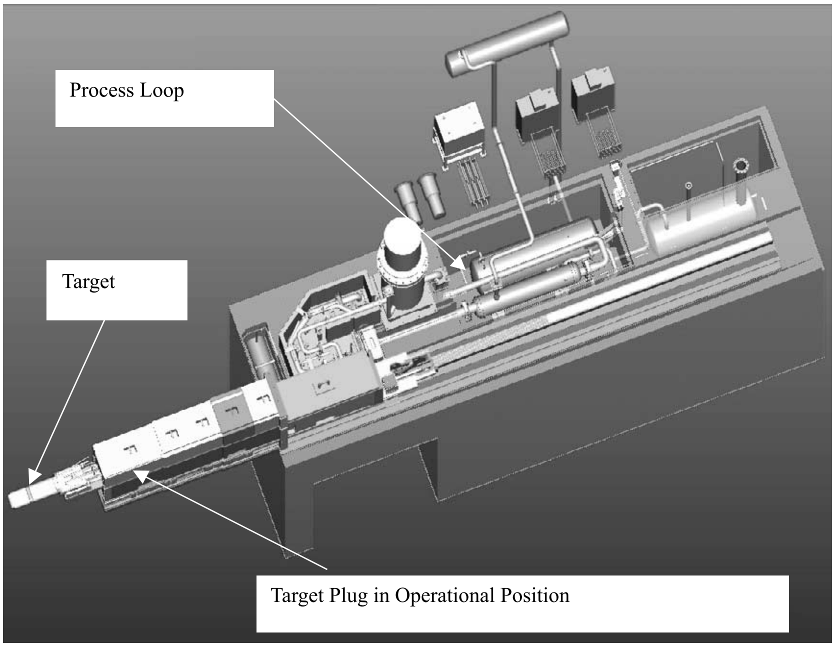

Fig. 3. The SNS target system, consisting of a stainless steel structure containing mercury, referred to as the target, a process loop, a means for moving the target module between its installed position and a hot cell, and moveable shielding in the target module's path between the hot cell and its installed position.

used for the window has significant structural advantages that help to sustain the other loads on the target. For example, a single monolithic structure made thick enough to sustain the internal pressure would have significantly higher operating temperatures and thermal stresses.

A separate outer shell, referred to as a shroud, is provided to contain mercury in case the mercury vessel fails. The shroud is also a double-walled structure cooled by water flowing between its two walls. The region be-

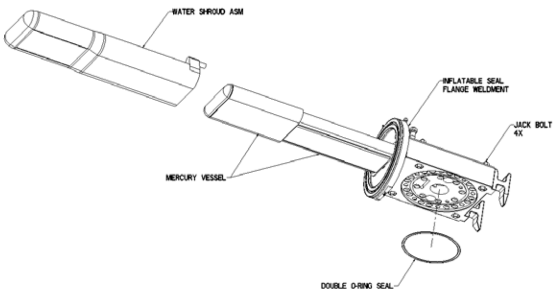

Fig. 4. The target module includes the mercury vessel, the water-cooled shroud, and seals mounted on a flange that forms the interface to the core vessel and process piping. The mercury target vessel is comprised of front and rear sections connected by flow tubes. The demarcation between the two sections is indicated by the two pointers over the words 'Mercury Vessel'.

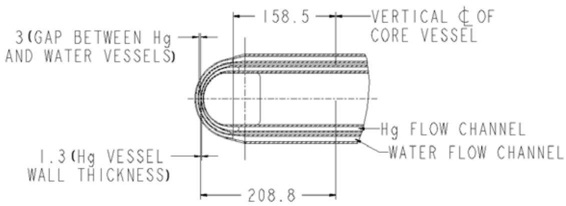

Fig. 5. A vertical center cross-section of the front end of the module parallel to the direction of the beam. A dedicated flow of mercury is directed between the walls of the mercury vessel in order to cool the target window, the portion of the vessel in the direct path of the proton beam. Numbers indicate corresponding lengths in millimeters.

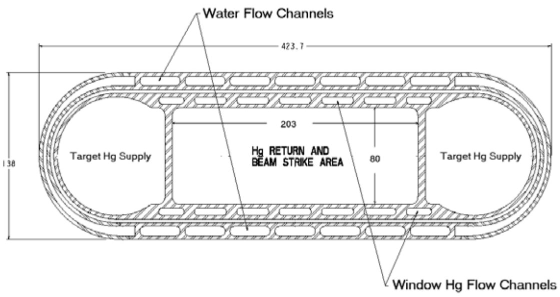

Fig. 6. A cross-section of the module perpendicular to the direction of the proton beam.

tween the shells is filled with helium and is monitored to detect leakage into it of either water or mercury.

The target module shell is being designed according to a structural criterion derived from the ASME Pressure Vessel Code. Loads during normal operation include those from vacuum, coolant pressure, from pressure waves due to thermal shock, component weights (gravity), and thermal effects. Off normal loads include those resulting from upsets within the target assembly system, other interfacing systems, as well as external events, such as seismic activity. Different stress criteria are applied to different events considering their probability and consequences of their occurrence consistent with the rules contained in the structural code. The effects of radiation are included when determining allowable material stresses in system structures. Replacement of the first target module is planned when a damage level of no more than 5 dpa is reached in the mercury target container.

The interaction of the energetic proton beam with the mercury target leads to very high heating rates in the target. Although the resulting temperature rise is only about 10°C, the rate of temperature rise is enormous ($\sim 10^7$°C/s) during the brief beam pulse of ~ 0.7 μs, which is repeated at a frequency of 60 Hz. The resulting thermal-shock-induced compression of the mercury leads to the production of large amplitude high-frequency pressure waves in the mercury that interact with the mercury target container and the bulk flow field. As a result of this effect, fatigue analysis is included in the design criteria. Temperature cycles due to beam trips and restarts also are considered in the fatigue analysis.

The Hg process system and the shroud cooling system are designed to absorb and transfer a combined power load of 1.2 MW. Approximately 20 tonnes of mercury flowing at 25 l/s maintains the peak temperature of the austenitic stainless steel target vessel to less than 200°C. This temperature limit was chosen to avoid dissolution of the nickel in the vessel material by the mercury, which circulates at temperatures between 60°C and 90°C.

4. Research and development program

R&D is crucial to the success of the SNS. It is being relied upon to provide the basic information needed to support engineering design of the facility so that it will meet the intended service. Ongoing work in the R&D program has formed a foundation for the target design described above. The program consists of interrelated activities in key disciplines to develop necessary experimental data, analyses and test demonstrations. The major tasks of the program are materials qualification, thermal performance, particle transport, and remote handling. The purpose of the present paper is to give an overview of the R&D program tailored to provide perspective on how the materials work fits into the overall plan. Other manuscripts from the SNS project in these proceedings [9–15] cover a range of recent activities and results in the materials portion of that effort. Here we incorporate some of those results by showing excerpts and by reference as necessary for the description.

The materials work interacts strongly with thermal performance as well as with particle transport studies. Work in the former area is summarized in Section 5. The particle transport work that most closely interacts with materials efforts is the calculation of displacement damage and transmutation production. These activities are covered in Section 6.1.

5. Thermal hydraulics and thermal shock R&D

The thermal performance program is aimed at defining a system that can remove the power deposited in the target without excessive temperatures or stresses. Ongoing development activities are focused on thermal hydraulics and thermal shock. To conduct these studies we are operating several flowing loops, performing tests at accelerator facilities, and benchmarking computer models. The thermal performance program is described in more detail in [16].

Work associated with the transport of the time-averaged power deposited by the beam is referred to as thermal hydraulics R&D. It is divided into four elements including: (1) computational fluid dynamics (CFD) simulation of the target, (2) mercury thermal hydraulic loop (MTHL) tests aimed at measuring fundamental fluid dynamic and heat transfer characteristics, (3) flow distribution tests using water as a surrogate fluid in a prototypical target configuration water thermal hydraulic loop (WTHL), and (4) full-scale mercury loop tests in a target test facility (TTF) with a prototypical mercury process loop and target geometry. These loops will provide the data to confirm that mercury can transport the deposited proton beam power away from the target, and can adequately cool the stainless steel target vessel. The data will also be used to benchmark the CFD model that will then be used as an engineering design and analysis tool.

The effort aimed at developing a target vessel and flow system that can withstand the pressure pulses resulting from the isochoric heating conditions in the target is designated thermal shock R&D. It includes: (1) fundamental pressure pulse and cavitation tests in off-line laboratories, (2) experiments at accelerator facilities using mercury target mockups, (3) computer modeling of thermal shock processes in the mercury target, and (4) evaluation of the long-term effects of these cyclic shock loads on the fatigue lifetime of the vessel. Initial laboratory and accelerator target tests have confirmed that the mercury is likely to undergo gaseous cavitation within the target, and that peak vessel stresses would be less than estimated using models that do not include the effects of cavitation. Future tests are designed to improve the understanding of this phenomenon as well as to investigate methods to mitigate the effects of the pressure pulses.

5.1. Thermal hydraulics

Several specific areas are being addressed. These include the wettability of liquid mercury on stainless steel surfaces with corresponding effects on heat transfer and frictional pressure drops, and the fluid flow characteristics of the bulk flow in the target and cooling jacket regions where the primary proton beam is depositing its energy.

5.1.1. Mercury thermal-hydraulic loop

Loop components were selected to provide measurements at prototypic heat flux levels, temperatures and flow rates corresponding to those in the passages of the target cooling jacket. A photograph of the MTHL facility is shown in Fig. 7. The facility is a closed piping loop, constructed primarily of 316 stainless steel, and designed to circulate liquid mercury at velocities representative of the target cooling jacket (~3.5 m/s). An electromagnetic pump with variable speed control provides the driving force for circulating the mercury. Mercury is stored in a supply tank located under the loop when the loop is not in operation. For operations, a helium gas overpressure is used to force the Hg through a standpipe into the loop and, in conjunction with helium overpressure in a level control tank located above the loop piping, to maintain system pressure during loop operations. Feedback control loops are used with helium supply and vent valve arrangements on the two tanks to maintain pressure in the system at the desired setpoint. The loop is instrumented for flow, temperature, and pressure measurements. A PC-based distributed control and data acquisition system is used for control functions and recording of measurements. Several test sections have been used in the mercury loop to provide the required data over a range of mercury inlet temperatures from 80°C to 200°C, mercury pressures from 0.1 to 0.4 MPa and velocities from 1 to 4 m/s. The measured nondimensional heat transfer data agree well with computational fluid dynamics calculations. All tests have achieved excellent heat transfer.

Fig. 7. Mercury thermal hydraulic loop (MTHL) used to study the heat transfer characteristics of mercury under a range of operating conditions.

Most recently, the MHTL is being converted to a materials test loop after the completion of its planned fluid dynamics and heat transfer tests. In this mode it will be used for high flow velocity tests to examine possible corrosion and mass transfer beyond what was observed in the low velocity tests mentioned in Section 6.4 and described in detail in [14].

5.1.2. Water thermal-hydraulic loop

This loop is being used to evaluate flow characteristics in the target bulk flow region, especially recirculation and stagnation regions. A full-scale mockup of the bulk flow region within the SNS target assembly has been fabricated using stereo lithography with a molding process to accurately model the interior design details. The front 0.59 m of the target is constructed of a clear urethane molded structure to provide access for flow visualization studies and velocity distribution measurements using a laser Doppler velocimeter (LDV). A photograph of the test section installed in the loop is shown in Fig. 8.

Test objectives for the WTHL include benchmarking of CFD codes, examination of the effect of design changes on the target fluid performance, and evaluation of diagnostic methods that may be applicable to mercury tests in the TTF described below. Measurements that are being made in the WTHL include flow rate for each inlet, pressure drop across the test section, pressure measurements at selected locations in the transparent front section, detailed local velocity vectors in the transparent section using a 2-D LDV system, and flow visualization studies using injected dyes and gas bubbles. Very good agreement between the CFD predictions and flow visualization results as well as LDV measurements of the flow field has been demonstrated.

5.1.3. Target test facility

This loop provides a full-scale test bed for confirmatory thermal-hydraulic tests using mercury. A photograph of the facility is shown in Fig. 9. The loop is constructed of type 304 and 316 austenitic stainless steels. The purpose of the thermal-hydraulic tests planned for this facility is to provide confirmation that the full scale target meets its design requirements with

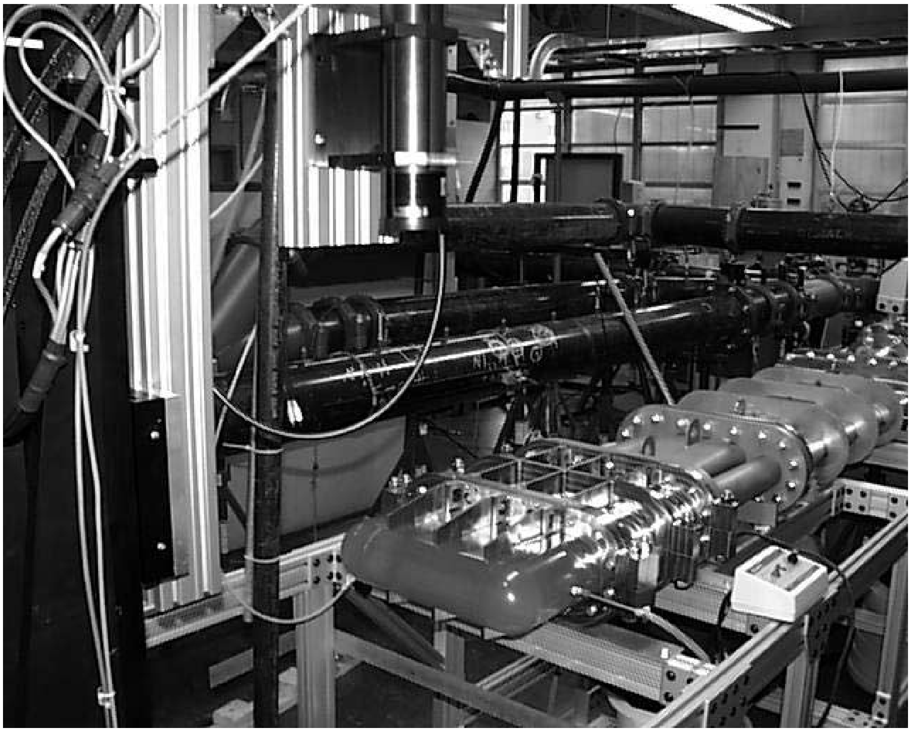

Fig. 8. Water thermal hydraulic loop (WTHL) used to study the overall characteristics of the bulk mercury flow in the SNS target.

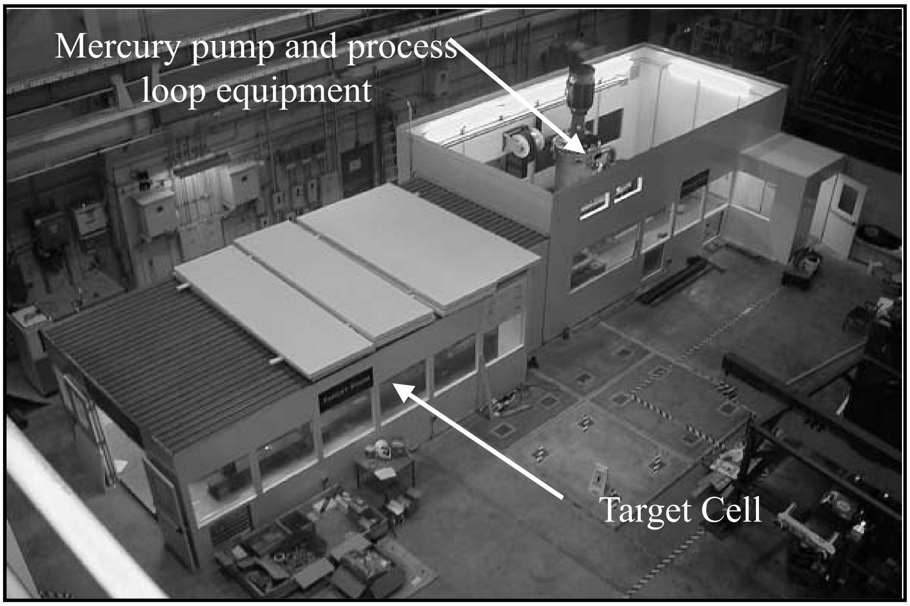

Fig. 9. Target test facility (TTF) is a full-scale prototype of the SNS mercury target flow loop.

mercury as the fluid. It is not practical to impose prototypic heat loads at this scale, so the tests and measurements will focus primarily on the hydraulic aspects of the target. Measurements of local wetting/non-wetting conditions and local heat transfer coefficients will be performed in limited areas of the target. In addition, CFD models previously benchmarked in the WTHL will be benchmarked for mercury.

Initial tests have been conducted to verify hydraulic performance of the pump and piping system, using a flow jumper in place of the target. Testing in this configuration was of limited scope and was used primarily to address general target flow supply questions. This included measurement of flow rate, flow splits, and pressures for confirmation of overall friction factors and pressure drops within the piping system. A second testing phase will use separate test sections to examine simultaneously, from a hydraulic standpoint, the bulk flow within the target and the flow in the target vessel cooling jacket at full scale. Again, data will be used to benchmark the CFD codes that are being used for design confirmation.

5.2. Thermal shock

A series of pulsed accelerator beam tests of several mercury target configurations have recently been completed at LANL in an attempt to gather the data needed to benchmark computer models used to predict thermal shock effects. Fiber-optic-based strain sensors have been developed to measure the response of the target vessel to the induced pressure waves in this intense radiation environment. Short pulses ($\sim$300 ns) of protons were obtained at the Weapons Neutron Research (WNR) facility at LANL to simulate the SNS environment. The energy density in the Hg was equivalent to that in the SNS but the modules irradiated were approximately half-scale. The notable aspects of the data collected during these tests were that the magnitude of the strain was relatively large, as predicted, while the frequency response was surprisingly low, which was not well predicted. A possible explanation is that cavitation of Hg caused by dissolved gas significantly changes the wave propagation, possibly due to changes in compressibility, or to scattering effects of gas bubbles. The most recent tests at the WNR facility have furnished substantial data on new test targets, which are expected to provide further insight into this issue.

6. Materials R&D

A main goal of the materials R&D program is materials qualification. This entails selection, testing, calculations, analyses, and feedback for improvements in materials and operating conditions to give confidence that key components will meet required service performance. At the same time, results of these activities help set initial lifetime and performance expectations for components, and help determine engineering limits that must be met by design provisions. The focus is on examinations of two aspects of the SNS environment that are considered to be particularly demanding: radiation effects and compatibility issues for structural materials of the target module. Past progress in materials R&D has been highlighted in our previous review papers [17–19], and in presentations whose records are available in the proceedings of the three earlier meetings of the series from which the present proceedings volume emanates [4–6].

The radiation effects activities consist of calculations and analyses, as well as irradiations in several actual and partially simulated spallation environments. Extensive post irradiation examinations are comprised of microstructural characterizations, mainly by transmission electron microscopy, and of mechanical property testing. The compatibility work addresses the dual issues of mass transfer corrosion for materials in contact with mercury, and effects of mercury on behavior in mechanical properties tests. Chemical wetting of structural materials may have a significant influence on both mass transfer and mechanical properties, and many of the compatibility experiments have included trial attempts to ensure wetting.

An activity that will take on heightened importance when the SNS begins operation in 2006 is the in-service surveillance program to monitor performance of structural materials in the actual environment. The knowledge gained will be fed back to the design and fabrication of future targets and to the evolution of operational procedures and lifetime estimates. Because provisions must be incorporated today in the design of the target region and in the service hot cell to accommodate the in-service surveillance program, we have already planned the work in some detail. It is planned to make use of both prefabricated miniaturized specimens that will be irradiated in the target, and of post-irradiation examinations of actual target containers and other service components. The miniature specimens are of standardized designs that will help the SNS benefit from the much larger database of measurements from irradiations in fission, fusion and basic research programs. At the same time, however, post-service examinations of actual SNS components are deemed to be irreplaceable in arriving at reliable performance limits and lifetime predictions for the facility. Such tests will not necessarily be based on standardized specimens because of such target specific features as curved geometries, non-optimum dimensions or special thermomechanical treatments, for example.

Other materials activities related to the R&D program provide technical support that is highly specific to the design of SNS. This technical support work usually takes the form of appropriate tests and analyses as needs arise. It differs in scope and purpose from the R&D program, which is based on a longer range plan to obtain systematic knowledge of materials performance in the spallation environment.

Most of the experimental activities being carried out in the materials R&D program are represented in Table 1. Listed across the top in abbreviated form are attributes of a spallation environment that we consider to be potentially important to the performance of a structural material. Listed down the left hand side are the types of experiments that we are carrying out to address these irradiation and compatibility factors. The top row of the table describes the SNS. As can be seen, a material in the SNS will experience all the conditions: high beam energy (GeV), high dose, high He transmutation rate, high H transmutation rate, contact with flowing mercury, irradiation of thick sections (millimeters, in contrast with the micrometer irradiated material thicknesses of some low-energy accelerator experiments), applied stress, and significant time variations in applied stress leading to fatigue. The following eight rows describe the types of experiments in the materials R&D program from the perspective of how many of the SNS attributes that they effectively address. An empty space in the table means that the corresponding experiment does not have the capability to address the corresponding attribute.

6.1. Radiation damage calculations

Calculations of radiation damage begin with the same particle transport calculations that are used to determine energy deposition for heat transfer considerations, shielding needs, and radioactivation of structural materials. Particle fluxes from these calculations are combined with cross-sections for displacement, He, and H production. Transmutation products in the stainless steel container [20] and in the mercury [21] are calculated by applying the proton and neutron fluxes to the appropriate transmutation cross-sections in a similar way. The most recent calculational work is described in manuscripts included in the present volume [9,10].

Table 2 gives the dpa, He and H production rates at the nose of the innermost shell of the target container. This shell is the wall of the container in Fig. 5 that is in contact with the bulk mercury target material on its concave side and with the coolant mercury in the passage on its convex side. The center of the nose is the location where the radiation damage is the highest, corresponding to a peak proton beam flux of approximately $0.22\ A/m^2$. In Table 2 it can be seen that the damage rate is 36 dpa for a full power year at 2 MW power, and that the He and H accumulate at rates of approximately 40 and 500 appm/dpa, respectively. Table 2 also reveals that about 2/3 of the displacement damage at this location is caused by neutrons and about 1/3 by protons. In contrast, the transmutations of He and H are dominated by the protons. The proton-induced displacements have He and H transmutation production rates per dpa that are between two and three times higher than the production rates per dpa for total displacements. It should be noted that while categorization into contributions from neutrons and protons is useful for certain analyses of proximate causes, all damage and transmutations are ultimately caused by the proton beam.

6.2. Spallation irradiations

Specimens for SNS have been irradiated at the LANSCE facility at LANL and at the SINQ facility at the Paul Scherrer Institute in Switzerland. Many of the specimens irradiated at LANSCE have been tested, and a summary of some key results is presented in a companion paper in this volume [11]. The SNS specimens

Table 1
Materials R&D experiment summary for SNS

Experiment	Attribute							
	Energy	Dose	He	H	Hg	Thick	Stress	Fatigue
SNS	High	High	High	High	Flow	[a]	[a]	[a]
TIF 3-beam	Low	High	High	High				
TIF p-beam	Low	Low			Flow		[b]	
LANSCE	High	High	High	High		[a]		
SINQ	High	High	High	High	Static[c]	[a]	[b]	
HFIR	Low	High	High			[a]		
TC loop					Flow	[a]		
LME tensile					Static	[a]	[a]	
LME fatigue					Static	[a]	[a]	[a]

The full scope of activities being carried out in the materials R&D program is summarized. Across the top in abbreviated form are attributes of a spallation environment that are potentially important to the performance of a structural material. Listed down the left-hand side are the types of experiments being carried out to address these irradiation and compatibility factors.[a] Typical for SNS.
[b] Possible relevance to SNS.
[c] A small fraction of the specimens exposed to Hg.

Table 2
Peak damage rates at front of target

	dpa/yr	appm He/yr	appm H/yr	He/dpa	H/dpa
Neutron	23	130	1800	5.7	78
Proton	13	1260	17 000	97	1310
Total	36	1390	18 800	39	522
p/n	0.57	9.7	9.4	17	16.8

Results calculated for displacement damage, He and H production rates at the innermost shell of the four-walled target container and shroud assembly. This is the wall of the assembly in contact with the bulk mercury on its inner surface and with the coolant mercury on the outer surface. The center of the nose is the location where radiation damage is highest, corresponding to peak proton beam flux of approximately 0.22 A/m^2.

irradiated at SINQ are a portion of a larger set irradiated as part of an international collaboration. This large experiment is described in detail in a paper contained in the present volume [22]. The first of these specimens are scheduled to be shipped to ORNL and to other laboratories in Europe and Japan for testing in the near future. Other specimens are now undergoing irradiation as part of a second round of experiments.

At LANSCE, a tungsten target was bombarded with a beam of 800 MeV protons at a current of 1 mA, with pulse frequency of 80 Hz and duration of 0.8 ms. The exposure period was 3614 h. A wide range of materials was irradiated either directly in the proton beam immediately in front of the target or in the mixed proton and spallation neutron field downstream of the target. Specimens were held in water-cooled stainless steel tubes at temperatures <164°C, and they reached maximum displacement doses of about 10 dpa for steels and about 20 dpa for heavier refractory metals. In addition to stainless austenitic and ferritic/martensitic steels, specimens of Ta, Ta-10 W, and Zircaloy-4 in annealed conditions were included to obtain data for possible future water-cooled solid spallation targets. Results for the refractory alloys will be published separately [23]. Overall descriptions of the LANSCE irradiations and facilities are available elsewhere [24,25].

Fig. 10 shows tensile stress/strain curves of SNS specimens that were irradiated at LANSCE. It is evident that the performance of the stainless steels is superior in retention of ductility with increasing dose to that of the other materials tested. However, data measured [26] on other 300 series steels irradiated at LANSCE indicate that uniform elongation may be reduced strongly by modest increases in the tensile test temperature. At the same time, fracture toughness data reported [27] for the same materials from the same irradiations show acceptable fracture toughness at 10 dpa.

We have made a careful assessment of the available data, and also have taken into consideration that there is no existing test bed from which to obtain data for materials irradiated in mercury under prototypical SNS conditions. This is illustrated in a compelling way by Table 1. The available data supports a plan to remove

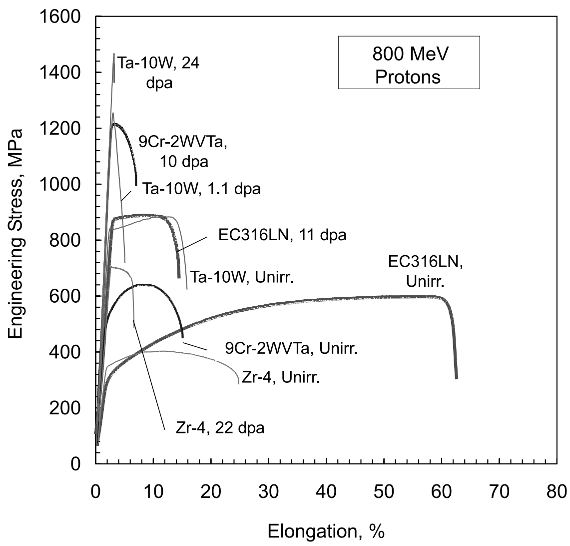

Fig. 10. Tensile curves for several materials irradiated in the LANSCE accelerator by a combination of 800 MeV protons and spallation neutrons. The irradiation temperature was <160°C for all specimens, and the maximum dose achieved was 24 dpa on the Ta-10 W alloy.

the first target after a peak dose of no more than 5 dpa. The target will be sectioned for post-irradiation mechanical property and microstructural examinations. Surveillance specimens of standard miniaturized configurations irradiated in selected locations within the target also will be examined. Based on the results of these examinations, estimates of target lifetime in the actual service environment will be refined, possibly resulting in recommendations for longer change out intervals for future targets.

6.3. Low-energy accelerator irradiations

The unique Triple Ion Facility at ORNL is being used in a variety of experiments to investigate salient aspects of the SNS irradiation environment. This facility has the capability to bombard a target simultaneously with three ion beams, as shown in Fig. 11. The facility

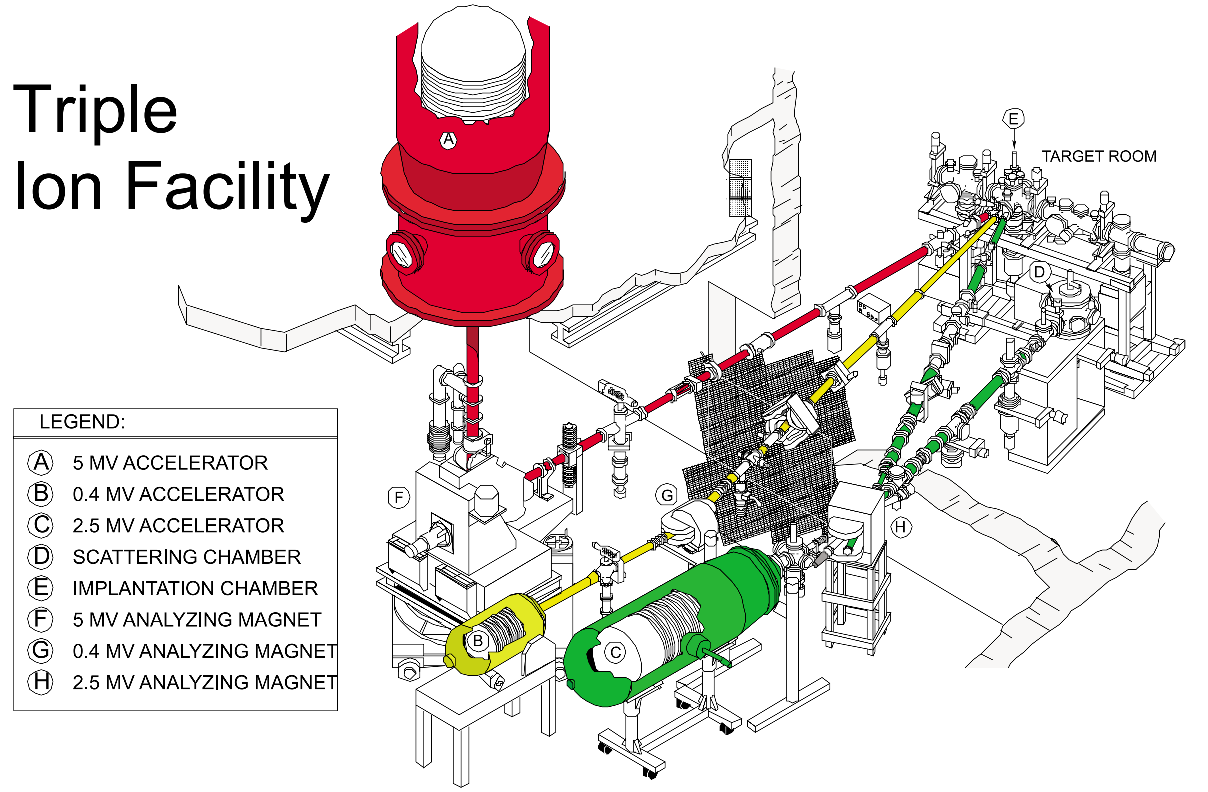

Fig. 11. Artist's representation of the ORNL triple ion facility (TIF). Three accelerators are configured so that a wide range of single, dual or triple ion beams can be applied simultaneously to a single target. For the SNS triple beam research the large accelerator is typically used for Fe-ions, with the intermediate accelerator for He-ions and the small accelerator for H-ions, in order to simulate aspects of the radiation damage and transmutation production in the spallation environment. For the irradiations in contact with liquids, the intermediate accelerator is used to accelerate a beam of H-ions. Also shown is a separate beamline where the chamber utilized for ion beam analysis is located.

utilizes Van de Graaff accelerators of terminal voltages 5, 2.5, and 0.4 MV. Typically the large accelerator is used to impinge a beam of Fe ions on the target, producing displacement damage rates in the range of 10^{-3}–10^{-2} dpa/s. As an aside, the rate of 10^{-2} dpa/s will be the rate of damage production at the highest damage region of the SNS target during a proton beam pulse, where the corresponding time-averaged rate would be 10^{-6} dpa/s. Using Fe ions has the virtue that these are self-ions of Fe-based alloys like austenitic stainless steels, so that impurities are not introduced and the composition of the steel is changed negligibly. The intermediate accelerator may be used to inject a He ion beam into the specimen at relative rates that mimic the spallation He/dpa rate. Similarly, the 0.4 MV accelerator may be applied to inject H into the specimen at spallation relevant rates.

Three areas currently under investigation at the accelerator facility cover: hardening by displacement damage and by the effects of the gases He and H; retention of implanted H in irradiated material; and radiation-induced interactions of structural materials with mercury and with water. The latter experiments employ a unique apparatus developed for this application, where a single proton beam passes through a foil window, the opposite side of which is in contact with the liquid. For investigations of hardening and associated microstructural changes the energies and currents of the beams are controlled so that representative He/dpa and H/dpa ratios, for example, are achieved within the first micrometer of the surface of the specimen. Current experiments utilize ratios at the high end of the range of the transmutation gas production rates in a spallation facility operating at 1 GeV. The hardening and microstructural results for single, dual and triple beam irradiations that are relevant to spallation conditions are described in [13] for Alloy 718 and in [28–30] for type 316LN stainless steel.

Hardening by He up to levels nearly a factor of two higher than could be produced by displacement damage alone was observed. High densities of He bubbles of nanometer scale were seen in TEM, along with evidence that the bubbles were serving as effective pinning centers for deformation dislocations [12]. However, hardening above the displacement-induced level was observed only where the He content exceeded 1 at.% [28]. Gas bubbles also were observed only above this level. It is important to note in this connection that He in SNS structural materials is not expected to reach this level within the target vessel lifetime. The level of approximately 1% required for excess hardening had been reported previously in ion beam irradiations [31], carried out under different conditions than the present experiments. In our experiments, H also was found to have an effect on hardening, though substantially less effect than He. In addition, much higher levels than expected of the injected H were retained, up to 50% or more, depending on temperature and other conditions. H is expected under normal conditions to diffuse easily in stainless steel at room temperature, leading to its loss at specimen surfaces. However, in irradiated material the H can be trapped by radiation-induced defect clusters and is strongly trapped in the presence of He [29,32]. Again, the hardening by H was found to occur at levels too high to be of concern for the SNS target. Although the hardening by these species was found to be negligible at SNS conditions, other mechanical property changes that He and H may induce, such as reductions of uniform elongation or fracture toughness, may be caused by SNS levels of these species. Investigation of such effects requires bulk-irradiated specimens, which are not produced in these low energy ion irradiations. Bulk effects are being investigated in the spallation irradiations described in Section 6.2.

Another type of experiment carried out at the accelerator facility is the irradiation of a thin foil specimen (15–20 μm) with a fully penetrating beam of protons. On the upstream side of the foil is the accelerator beam line vacuum. On the other side of the foil is flowing Hg or water. The proton beam, after passing through the foil, enters the fluid with enough energy (~0.5 MeV) to cause ionization and displacement interactions with water or Hg. Thus, water suffers large changes in chemistry caused by radiolysis, becoming more oxidizing, for example [33] and Hg (and its spallation products in the actual case) may be injected into the structural material causing changes in near surface properties and increases in displacement damage [10]. The purpose of these experiments is to investigate compatibility processes in conjunction with irradiation. Referring to Table 1, it is seen that there is no other experiment in the current program that investigates this essential feature of the SNS environment. (As noted in the Table, the experiment now being irradiated in SINQ includes three small capsules containing Hg in contact with specimens, but the Hg is static and its volume is the order of only 1 cm^3, suppressing possibilities for dynamic interactions.) This experiment, albeit employing MeV rather than GeV energy protons, is arguably more prototypic than the other experiments of Table 1, because they investigate either radiation effects or compatibility issues but not both together. A recent publication describes the proof-of-principle experiments that established the irradiation technique in contact with fluid [34]. More recently, pronounced formation of an oxide film on an irradiated stainless steel surface in contact with flowing water has been observed after 5 dpa. In an even more recent experiment, which has not yet been analyzed completely, strong oxidation of an irradiated stainless steel surface in contact with flowing Hg was observed after 5 dpa, in addition to other changes [35].

It should be noted that the absence of capabilities for proton irradiations of large scale flowing liquid metal loops containing specimens under stress is expected to change shortly. A facility termed the liquid solid reaction (LiSoR) experiment is under design and fabrication at the PSI [36]. The first experiments will utilize a lead bismuth liquid metal mixture in the loop, in connection with needs for future liquid metal target systems at the SINQ, and for investigations applicable to accelerator transmutation of waste technology.

6.4. Hg flow loop experiments

The compatibility testing program is carried out in the laboratory in the absence of irradiation. Work consists of two distinct types of investigations: generalized corrosion and mass transfer; and effects of Hg on mechanical properties of structural materials [14,15,19]. In the present section we describe the work to assess generalized corrosion and mass transfer. One of the issues motivating this work is the potential for loss of material and consequently compromised structural integrity of components in contact with Hg. The most likely issue is judged to be temperature gradient mass transfer. In this process, dissolution of the container material could occur, usually through preferential dissolution of one or more of the main compositional elements. Material dissolves in the liquid in relatively high temperature, i.e., high solubility, regions. This is accompanied by deposition of the dissolved material in relatively low temperature regions. As a result, corrosion of the high temperature region is not limited by system equilibrium and potentially may be accelerated over what would be experienced in an isothermal or static system. In addition to accelerated dissolution and possible loss of structural integrity in the hot regions, deposition of solute in the cold regions could conceivably cause flow disruptions and even plug piping. Such occurrences have been observed in liquid metal flow loops in the past. For this work a series of tests in Hg environments are being carried out.

The devices used in these experiments are thermal convection loops (TCLs). Here, one leg of a piping circuit is heated and the other is cooled, resulting in a temperature gradient and a modest flow rate of about 1 m/min. Fig. 12 shows a photograph of one of the loops employed. Many copies of this loop have been run to investigate both 316 type stainless steels and Inconel 718 under different surface treatment conditions and different Hg environments. At the expected SNS operating temperatures, less than 200°C, pure mercury does not chemically wet stainless steel readily. Without chemical wetting, characterized by a low contact angle between a mercury droplet and the material surface, potential corrosion processes are inhibited. However, factors that may influence wetting in the actual SNS target to make wetting more likely include the presence of thermal hot spots and radiation damage. Creation of fresh oxide-free surfaces could result from potential flow cavitation and from pressure waves created by thermal transients resulting from beam pulses. To examine potential worst case corrosion, it is desirable to develop wetting in the tests for material compatibility with flowing mercury. Therefore, the thermal convection loop (TCL) tests in this program utilized peak temperatures near 300°C to achieve some amount of wetting. In addition, small amounts of Ga (up to 1000 wppm) were added to the Hg in some tests in an attempt to increase the tendency of the liquid metal to wet the loop containment and test coupons.

In tests to date, austenitic type 316L and 316LN stainless steels have been exposed to flowing Hg at velocities of 1–5 m/min in thermal convection loops at temperatures up to 305°C for periods up to 5000 h. A wide variety of surface treatments were employed, including: gold-plated, polished, implanted with Fe to 40 dpa, oxidized, acid-etched, machined, welded, and sensitized. Wetting by Hg under the conditions examined was not found to be particularly uniform or predictable, although high Hg temperatures, gold-coating of specimens, and steam cleaning of surfaces prior to exposure all seemed to encourage wetting, while addition of Ga was found to be ineffective in this regard.

In the cases of observed maximum interaction with Hg, a porous layer substantially depleted in Ni and Cr formed at the exposed surface, leading to transformation of the affected area to ferrite. More often, only slight surface roughness developed on mercury-wetted specimens. Among all of the test exposures, heat treatments, and surface conditions examined, the maximum penetration was observed to correspond to about 60–70 μm/yr on a gold-coated surface. On a steam cleaned surface the maximum penetration was about 15 μm on a 316L coupon exposed for 5000 h. Fig. 13 shows the results of an electron beam analysis of this specimen, which found that Fe was enriched and Ni and Cr were

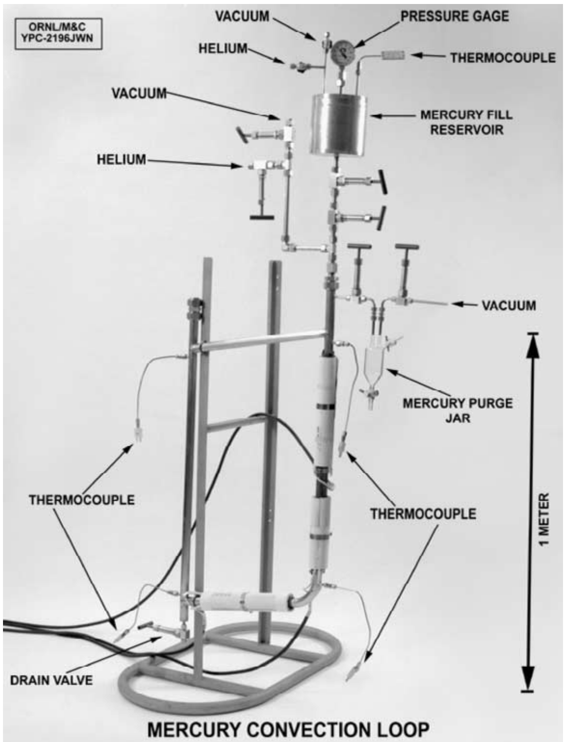

Fig. 12. Thermal convection loop used for temperature gradient mass transfer investigations of type 316 stainless steel and Inconel 718. The hot leg, where heater sections can be seen on the right, was typically run at 305°C in the hottest region, and the cold leg on the left was typically run at 240°C in the coldest region.

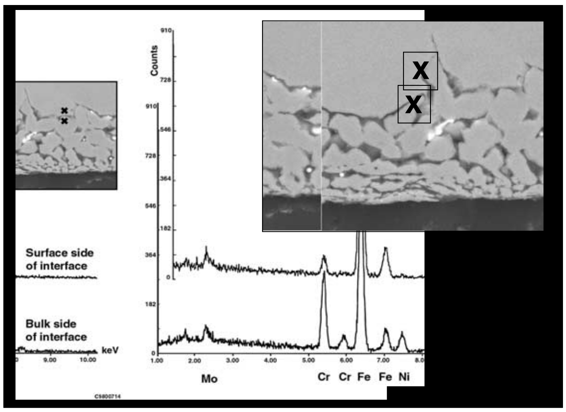

Fig. 13. Scanning electron micrograph of a cross-section from a 316L coupon exposed for 5000 h in a Hg thermal convection loop of the type shown in Fig. 12. The accompanying electron beam analysis shows that the base material, at the upper 'X' (about 15 μm into the coupon from the corrosion front), contains normal proportions of Ni and Cr for the alloy. However, the material on the mercury side of the corrosion front, at the lower 'X', is devoid of Ni and Cr peaks, indicating that these elements have been depleted from the alloy by exposure to Hg.

depleted in the surface region exposed to Hg. Alloy 718 was also investigated in similar type loops for temperature gradient mass transfer. It was found to be essentially immune to Hg interaction under the more limited set of conditions to which it was exposed. No deposition of dissolution or corrosion products was observed in the cold leg of any of the loops. However, some dissolution products in the form of oxides were recovered from the mercury when the loops were drained.

Additional tests are planned for the near future in a special materials test section inserted into the forced convection flow loop designated as MTHL and described in an earlier section, which will expose coupons to Hg flowing at velocities above 1 m/s. These velocities will be close to that in the maximum flow rate region of SNS and will help answer questions about how high velocities may affect wetting and material removal.

6.5. Mechanical properties tests

The other type of compatibility testing being pursued in the SNS materials R&D program concentrates on possible effects of Hg on mechanical properties of the structural material. Hg could conceivably change mechanical properties by affecting grain boundaries, for example. For these investigations a series of mechanical property tests is being carried out in air and in Hg.

In the earliest of these tests, U-bends of stainless steel were immersed for varying periods in Hg baths. The U-bend ensures that the material is deformed past its yield stress so that surface films may be broken and grain boundaries will be forced to slide, with the idea that the material may be made more susceptible to attack. No differences were found between U-bends exposed to Hg while being held at stress and control specimens in air. Next, a series of tensile tests was carried out in air and Hg. Some tests were stopped after the yield stress was exceeded, and then continued to failure after several weeks. In all the tests, with 316L and Inconel 718 in different starting thermomechanical treatment conditions, no significant differences in yield stress, ultimate tensile stress or uniform elongation were observed.

One of the considerations in the lifetime of the mercury target arises from the fact that the beam is pulsed, as described above. There are also other time-varying stresses applied to the container at lower frequencies. For example, in routine operation of large accelerators there can be multiple beam trips per day from various causes, whose durations may last from fractions of a second to much longer times in some cases. In addition, normal startup and shutdown will result in temperature and stress transients applied to the target container.

For these reasons it is considered important to obtain fatigue test information on the target container structural material. Since the magnitudes and frequencies of the expected stresses vary substantially, we have developed a fatigue testing program to generate full applied stress vs cycles-to-failure plots [15,37,38]. The information is being obtained both for specimens immersed in mercury and for specimens in air. Even at 60 Hz, i.e., not considering the secondary pressure pulse 'ringing' following the initial pulse, a large number of cycles will be accumulated during operation. In some tests a high-frequency fatigue machine, running at 700 Hz, has been used to enable the rapid achievement of 10^9 cycles, corresponding to about 6 months of proton pulses at 60 Hz. Testing is being carried out over a range of parameters to determine the effects on fatigue lifetime of alternating stress magnitude, *R*-ratio (minimum to maximum stress ratio), frequency, waveform, and temperature, for example.

Fig. 14 is a summary plot of some of the information obtained to date. Tests in air and mercury are shown, with alternating stress plotted against cycles to failure for $R = 0.1$. Tests in air were carried out at two different frequencies, 10 and 700 Hz. At high stress-low cycles to failure, the specimens tested at 10 Hz displayed a significantly longer lifetime than those at 700 Hz. When temperatures were measured it was found that the high-frequency specimens tested in air were being heated by plastic deformation to temperatures as high as 270°C. It was confirmed that the shorter lifetimes at high frequency were caused by effectively testing the specimens at higher temperatures. The square points in the figure show the results of testing in mercury at 700 Hz. At high stress-low cycles the lifetimes were somewhat shorter than for low-frequency air tests but longer than the high-frequency air lifetimes. The improvement in life-

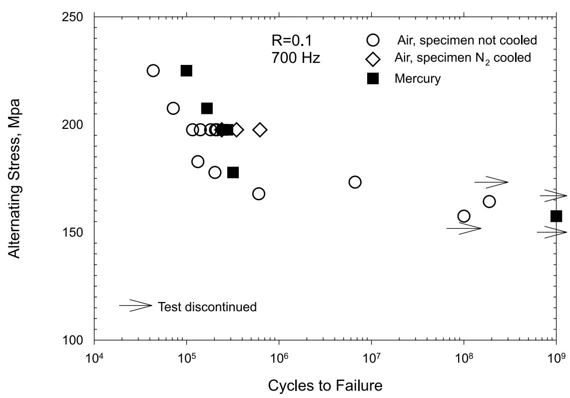

Fig. 14. Plot of alternating stress vs cycles to failure for specimens tested in air and in Hg at a frequency of 700 Hz and *R*-ratio of 0.1. It was found that the specimens in air had a shorter fatigue life than those in Hg. However, this was an artifact since the Hg acted to cool the specimens. When the specimens in air were cooled with gas evaporating from a liquid nitrogen bath, the lifetimes in air and Hg were comparable. Arrows connected to a data point indicate that the specimen did not fail up to the termination of the test at the indicated number of cycles.

time over air tested specimens for the high stress, high-frequency specimens in mercury is attributed to the cooling effect of mercury, which held the test temperatures of the specimens in mercury to 78°C and below. At alternating stresses somewhat below 170 MPa in Fig. 14, the specimens tested in mercury did not fail up to 10^9 cycles. The achievement of 10^9 cycles in mercury and similar high cycles in air indicates that there is little effect of mercury on fatigue lifetime at this stress level and below.

Other tests were conducted by fully reversing the load during the testing cycle, $R = -1$. At high stress amplitudes, i.e., considerably above the endurance limit of type 316LN SS, fatigue life in mercury was lower than in air by a factor of 2–3. In a report covering the high stress-low cycle regime [39], increased cracking and shorter lifetime in mercury than in air for tests at low frequency were attributed to liquid metal embrittlement. Those stresses were well above the yield stress of the material. When a fatigue crack is initiated, wetting by mercury of the clean, newly formed surface may occur, and subsequent crack growth rate could, therefore, be affected. However, because stresses must be kept below the yield stress by design during SNS operation, such a process would not be operable. An additional possible benefit in this context is that yield stress generally increases by two to three times when materials like stainless steels are irradiated even to low doses [11].

Future plans include fatigue crack growth tests and determinations of the effects of technical issues such as load control vs strain control of the applied stress. It is also planned to examine the effects of stress state by carrying out biaxial tests on disk specimens, in addition to the above-described uniaxial tests on cylindrical specimens.

7. Summary

The SNS is a collaborative project of six major laboratories in the USA. When completed it will be the most powerful accelerator-based source for neutron scattering research. The project is being managed by Oak Ridge National Laboratory, which is also responsible for designing the target systems of the facility. Construction is underway at a site in Oak Ridge, TN. Completion of the facility and startup of operations are expected in 2006. A research and development program was instituted at the inception of conceptual design in 1995. Early in the R&D program, liquid mercury contained within a multiple-walled structure was chosen as the spallation target. This is a creative choice that offers a number of advantages over a more conventional water-cooled solid target.

The purpose of the R&D program is to ensure that the maximum scientific and technical information is obtained in the early stages of the project so that the engineering design required to meet neutronic performance objectives of the scattering facilities can be attained. At the earliest stages of the conceptual design an aggressive materials R&D effort was begun. It has focussed mainly on the irradiation performance and Hg compatibility behavior of structural alloys for the target container. The prime candidate material is type 316LN austenitic stainless steel, whose choice itself was a product of the materials R&D program. Irradiations have been carried out both at available spallation facilities and at facilities that simulate some aspects of spallation environments, including the TIF low energy multiple beam accelerators and the HFIR fission reactor. The compatibility work consists mainly of mechanical properties tests in Hg and investigations of temperature gradient mass transfer in a liquid mercury environment. There is no available prototypical environment that we know of in which both spallation irradiation and Hg compatibility processes can be investigated under high flow rate conditions. However, some studies are included to investigate these combined processes by innovative experimental simulations in environments that are not prototypical. The results of the work to date indicate that the target design and materials performance will achieve their service goals.

Acknowledgements

Research was sponsored by the Division of Materials Sciences and Engineering, Office of Basic Energy Sciences, US Department of Energy, under contract No. DE-AC05-00OR22725 with UT-Battelle, LLC.

References

[1] G.S. Bauer et al. (Eds.), The ESS Technical Study, The European Spallation Source Study, vol. III, The ESS Council, ESS-96-53-M, ISBN 090 237 659, 1996.
[2] H. Lengeler, The European Spallation Source study (ESS), in: Proceedings of the ICANS-XIII Conference, PSI Proc. 95-02, ISSN 1019-6447, 1995, p. 819.
[3] The National Spallation Neutron Source conceptual design report, Oak Ridge National Laboratory Report, NSNS/CDR-2/V1 and NSNS/CDR-2/V2, May 1997.
[4] L.K. Mansur, H. Ullmaier (Eds.), Proceedings of the International Workshop on Spallation Materials Technology, Oak Ridge, TN, April 23–25, 1996, Oak Ridge National Laboratory Report, CONF-9604151, 1996.
[5] F. Carsughi, L.K. Mansur, W.F. Sommer, H. Ullmaier, in: Proceedings of the Second International Workshop on Spallation Materials Technology, Ancona, Italy, September 19–22, 1997, Forschungszentrum Jülich Report, Jül-3450, 1997.

[6] W.F. Sommer, H. Ullmaier, L.K. Mansur (Eds.), Proceedings of the Third International Workshop on Spallation Materials Technology, Santa Fe, NM, April 29–May 4, 1999, Los Alamos National Laboratory Report, LA-UR-00-3892, 1999.

[7] W.F. Sommer, T.O. Brun, L.L. Daemen, L.S. Schroeder, organizers, Materials for Spallation Neutron Sources, Los Alamos National Laboratory, February 6–10, 1995.

[8] B.R. Appleton, G.S. Bauer, in: Proceedings of the International Workshop on the Technology and Thermal Hydraulics of Heavy Liquid Metals, Schruns, Austria, March 24–29, 1996, Oak Ridge National Laboratory Report, CONF-9603171, June 1996.

[9] M.H. Barnett, M.S. Wechsler, D.J. Dudziak, L.K. Mansur, B.D. Murphy, these Proceedings, p. 54.

[10] Y. Zheng, M.S. Wechsler, D.J. Dudziak, J.D. Hunn, L.K. Mansur, these Proceedings, p. 61.

[11] K. Farrell, T.S. Byun, these Proceedings, p. 129.

[12] E.H. Lee, T.S. Byun, J.D. Hunn, K. Farrell, L.K. Mansur, these Proceedings, p. 183.

[13] J.D. Hunn, E.H. Lee, T.S. Byun, L.K. Mansur, these Proceedings, p. 203.

[14] S.J. Pawel, J.R. DiStefano, E.T. Manneschmidt, these Proceedings, p. 210.

[15] J.P. Strizak, J.R. DiStefano, P.K. Liaw, H. Tian, these Proceedings, p. 225.

[16] T.A. Gabriel et al., Nucl. Technol. 132 (2000) 49.

[17] L.K. Mansur, J.R. DiStefano, K. Farrell, E.H. Lee, S.J. Pawel, M.S. Wechsler, in: Proceedings of the Topical Meeting on Nuclear Applications of Accelerator Technology held at the American Nuclear Society Winter Meeting, Albuquerque, New Mexico, November 16–20, 1997, American Nuclear Society, La Grange Park, IL, 1997, p. 301.

[18] L.K. Mansur, in: Proceedings of the American Nuclear Society Meeting, Boston, MA, June 6–10, 1999, TANSAO 80, 1999, p. 94.

[19] S.J. Pawel, J.R. DiStefano, L.K. Mansur, K. Farrell, J.P. Strizak, T.S. Byun, in: Proceedings of the Topical Meeting on Accelerator Applications held at the American Nuclear Society Winter Meeting, Long Beach, CA, November 14–18, 1999, American Nuclear Society, La Grange Park, IL, 1999, p. 117.

[20] M.H. Barnett, MSc thesis, Department of Nuclear Engineering, North Carolina State University, April 26, 1999.

[21] M.S. Wechsler, Plot of transmutations in mercury irradiated by I GeV protons, private communication.

[22] Y. Dai, G.S. Bauer, these Proceedings, p. 43.

[23] T.S. Byun, K. Farrell, in: Proceedings of the Fourth Topical Meeting on Nuclear Applications of Accelerator Technology (AccApp 00), Washington, D.C., November 13–15, 2000, American Nuclear Society, La Grange Park, IL, 2001, p. 270.

[24] S.A. Maloy, W.F. Sommer, in: Proceedings of the Topical Meeting on Nuclear Applications of Accelerator Technology held at the American Nuclear Society Winter Meeting, Albuquerque, New Mexico, November 16–20, 1997, American Nuclear Society, La Grange Park, IL, 1997, p. 58.

[25] G.J. Wilcutt et al., in: Proceedings of the Second International Topical Meeting on Nuclear Applications of Accelerator Technology, Gatlinburg, TN, September 20–23, 1998, American Nuclear Society, La Grange Park, IL, 1998, p. 254.

[26] S.A. Maloy et al., The effect of high energy protons and neutrons on the tensile properties of materials selected for the target and blanket components in the Accelerator Production of Tritium project, in: Proceedings of the Twentieth International Symposium on the Effects of Radiation on Materials, ASTM STP 1405, American Society for Testing and Materials, in press.

[27] S.A. Maloy et al., in: Proceedings of the Winter Meeting on Accelerator Applications held at the American Nuclear Society Topical Meeting, Long Beach, CA, November 14–18, 1999, American Nuclear Society, La Grange Park, IL, 1999, p. 541.

[28] E.H. Lee, J.D. Hunn, N. Hashimoto, L.K. Mansur, J. Nucl. Mater. 278 (2000) 266–272.

[29] J.D. Hunn, E.H. Lee, T.S. Byun, L.K. Mansur, J. Nucl. Mater. 282 (2000) 131.

[30] E.H. Lee, J.D. Hunn, T.S. Byun, L.K. Mansur, J. Nucl. Mater. 280 (2000) 18.

[31] H. Ullmaier, E. Camus, J. Nucl. Mater. 251 (1997) 262.

[32] B.M. Oliver et al., in: M.L. Hamilton, A.S. Kumar, S.T. Rosinski, M.L. Grossbeck (Eds.), Proceedings of the Nineteenth International Symposium on the Effects of Radiation on Materials, ASTM STP 1366, American Society for Testing and Materials, 2000, p. 1109.

[33] S.M. Bruemmer et al., J. Nucl. Mater. 274 (1999) 299.

[34] M.B. Lewis, J.D. Hunn, J. Nucl. Mater. 265 (1999) 325.

[35] J.D. Hunn, M.B. Lewis, Observations of irradiated stainless steel in contact with Hg, to be submitted for publication.

[36] G.S. Bauer, Y. Dai, Plans for the LiSoR experiment, private communication.

[37] H. Tian, J.T. Broome, J.P. Strizak, P.K. Liaw, D. Fielden, L. Jiang, B. Yang, H. Wang, C.R. Brooks, L.K. Mansur, J.R. DiStefano, K. Farrell, D.C. Lousteau, S.J. Pawel, G.T. Yahr, Influence of mercury environment on fatigue behavior of spallation neutron source (SNS) target container materials, in: Proceedings of Prof. Campbell Laird Symposium, TMS Annual Meeting, Nashville, TN, March 13–16, 2000, Materials Science and Engineering, in press.

[38] H. Tian, J.T. Broome, P.K. Liaw, H. Wang, D. Fielden, L. Jiang, B. Yang, C.R. Brooks, J.P. Strizak, L.K. Mansur, J.R. DiStefano, K. Farrell, S.J. Pawel, G.T. Yahr, Effects of frequency and specimen self-heating on the fatigue life of 316 LN stainless steel, in: Proceedings of TMS/ASM Fall Meeting, Symposium on Fatigue and Fracture Behavior of High Temperature Materials, St. Louis, MO, October 8–12, 2000, to be published.

[39] S.J. Pawel, J.R. DiStefano, J.P. Strizak, C.O. Stevens, E.T. Manneschmidt, Screening test results of fatigue properties of Type 316LN stainless steel in mercury, Oak Ridge National Laboratory Report, ORNL/TM-13759, SNS/TSR-0097, March 1999.